Improved 1D-Var Assimilation Retrieval of Temperature and Humidity From the Ground-Based Microwave Radiometer Data

Observations Department,
Japan Meteorological Agency

Abstract

One-Dimensional Variational (1D-Var) assimilation retrieval is one of the optimal estimation methods to retrieve the atmospheric state from the brightness temperatures measured with a ground-based microwave radiometer. In this study, some adjustments are made in the 1D-Var calculation process as follows.

1. Bias correcting for the measured brightness temperatures ($T_{b[obs]}$).
2. Calculating the error covariance matrices of the microwave radiometer observation data and backgrounds (the short-range forecast data) in detail.
3. Including the surface observation data (temperature and specific humidity) into the 1D-Var calculation process.

Temperature profiles and specific humidity profiles retrieved under clear sky condition by using the improved 1D-Var method were statistically better than background profiles at altitudes of about 0-3 km and 0-4 km respectively.

1. Introduction

1D-Var assimilation retrieval from the brightness temperatures measured with the ground-based microwave radiometer has been discussed in the Observations Department, Japan Meteorological Agency. Yoshimoto (2007) retrieved vertical profiles from the measured brightness temperature ($T_{b[obs]}$) obtained in Naha from June 13, 2006 to June 30, 2006 using the 1D-Var method, and indicated that the accuracy of those profiles was statistically better than that of background at altitudes of 1-2 km in temperature. However, those profiles could not give positive impact in the case study of the numerical weather prediction (NWP) experiment with the mesoscale model (MSM) (Kawano, 2007). In addition, it was clarified that some improvements were necessary to the 1D-Var calculation process. This study intends to improve the 1D-Var calculation process, and evaluates the accuracy of vertical profiles retrieved by the improved 1D-Var method.

1-1. Ground-based microwave radiometer

This study uses the observation data from the Radiometrics microwave radiometer TP/WVP-3000. The radiometer has seven channels in the oxygen band 51-59 GHz and five channels between 22-30 GHz near the water vapor band, and obtains the brightness temperatures ($T_{b[obs]}$) every one minute. This radiometer also includes sensors to measure pressure, temperature, relative humidity on the surface, and zenith infrared temperature (T_{IR}). This radiometer was operated at several sites near Radiosonde launch sites for the periods listed in Table.1-1.

	Radiometer observation site	Latitude/Longitude	Observation periods	Radiosonde observation site (WMO index number)
1	Tsukuba	36˚03'N / 140˚08'E	04/19/06 - 05/26/06	TATENO (47646)
2	Naha	26˚12'N / 127˚41'E	06/06/06 - 07/07/06	NAHA (47936)
3	Sendai	38˚16'N / 140˚54'E	07/18/06 - 01/09/07	SENDAI (47590)
4	Tsukuba	36˚03'N / 140˚08'E	01/12/07 - 01/30/06	TATENO (47646)

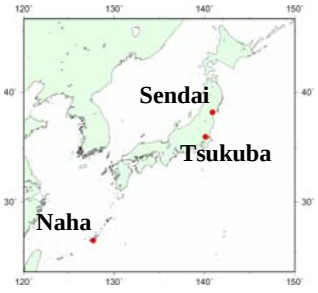

Table.1-1. Radiometer observation sites and radiosonde observation sites.

1-2. One-dimensional variational assimilation retrieval

1D-Var assimilation retrieval is thought to be one of the optimal estimation methods to retrieve the atmospheric state that is statistically most consistent with the radiometer observation data and background field from a short-range forecast. The 1D-Var method is performed by adjusting the atmospheric state vector, $\mathbf{x}$, to minimize cost function $J(\mathbf{x})$ defined as Eq.(1,1),

$$J(\mathbf{x}) = \frac{1}{2}\left(\mathbf{x}-\mathbf{x}^b\right)^T \mathbf{B}^{-1}\left(\mathbf{x}-\mathbf{x}^b\right) + \frac{1}{2}\left(H\mathbf{x}-\mathbf{y}^o\right)^T \mathbf{R}^{-1}\left(H\mathbf{x}-\mathbf{y}^o\right) \quad . \quad (1,1)$$

where, $\mathbf{x}^b$, $\mathbf{y}^o$, $\mathbf{B}$, $\mathbf{R}$, and $H(\mathbf{x})$ are the background state vector, the observation vector, the error covariance matrix of $\mathbf{x}^b$, that of $\mathbf{y}^o$ and the radiation transfer model operator transforming the atmospheric state vector into the observation vector, respectively. In the present study, the short-range forecast by MSM initiated six hours before the observation is used for $\mathbf{x}^b$. The brightness temperatures $T_{b[obs]}$ obtained from the radiometer are averaged during three minutes and are used for $\mathbf{y}^o$. The fast radiation transfer model provided by Ishimoto (2006) of the Meteorological Research Institute is used for $H(\mathbf{x})$ to calculate T_b in 12 channels from the vertical temperature and specific humidity profiles consist of 69 layers interpolated from the grid point values (GPV) forecasted by MSM.

2. Improving the 1D-Var calculation process

2-1. Correcting biases of the $T_{b[obs]}$

In the 1D-Var calculation process, it is assumed that $\mathbf{x}^b$ and $\mathbf{y}^o$ have no bias from the true value, and that the errors of $\mathbf{x}^b$ and $\mathbf{y}^o$ from the true value are based on the normal distribution. However, there are some biases between $T_{b[obs]}$ and $T_{b[sonde]}$, actually (Fig.2-1). Here, $T_{b[sonde]}$ are the brightness temperatures calculated from radiosonde profiles by using radiation transfer model, $H(\mathbf{x})$. For the improvement of the 1D-Var calculation process, it is necessary to correct these biases between $T_{b[obs]}$ and $T_{b[sonde]}$.

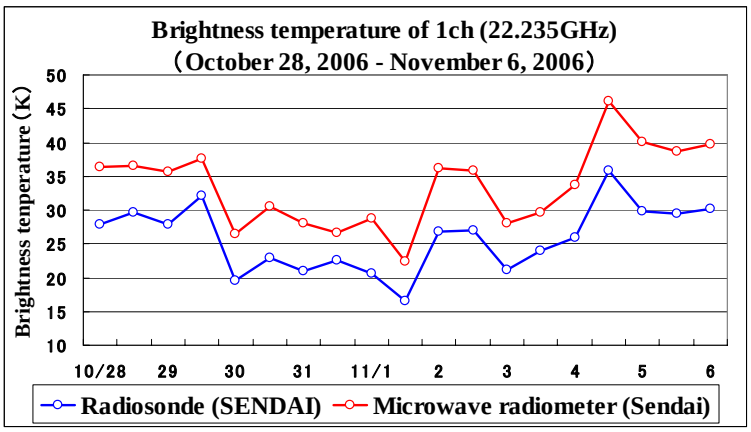

Fig.2-1. Biases between $T_{b[obs]}$ and $T_{b[sonde]}$ in one channel during 2006/10/28～11/06.

Yoshimoto (2007) calculated the brightness temperatures using analyzed profiles from 4D-Var for MSM ($T_{b[anal]}$) assumed as true values instead of the radiosonde profiles, and corrected biases of the $T_{b[obs]}$ using some periods' average values of the difference between $T_{b[obs]}$ and $T_{b[anal]}$. However, these average values are variable depending on the periods. It is necessary to correct biases of the $T_{b[obs]}$ without depending on the periods. Then, the scatter diagrams of each channel were made by using 399 cases at 0:00 UTC and 12:00 UTC from April 19, 2006 to January 30, 2007. Under cloudy weather condition or rain weather condition, the radiometer observes microwave radiation not only from the atmosphere but also from liquid water, and $T_{b[obs]}$ are much larger than $T_{b[sonde]}$. Then, only 160 cases under clear sky condition were selected. 72 cases were rejected as under rain condition by the rain detector equipped on the radiometer, and the other rejected 167 cases were considered to be under cloudy weather condition by the value of T_{IR} and liquid water path (LWP) retrieved by the water vapor channels. The criteria are given by Eq.(2,1).

$$T_{IR} \geq 263K \quad or \quad LWP \geq 0.1 \quad . (2,1)$$

22 of selected 160 cases are rejected as unexpected value because the difference between $T_{B[obs]}$ and $T_{B[sonde]}$ is larger than twice of standard deviation in one of 12 channels. The regression lines of each channel were drawn by using the other 138 cases (Fig.2-2). Using the regression lines for the bias correcting, it makes possible to correct biases of the $T_{B[obs]}$ instantaneously. This method also corrects biases of the $T_{B[obs]}$ obtained in any sites, once the regression lines are determined.

2-2. Observation error covariance matrix

Yoshimoto (2007) defined only diagonal components of the observation error covariance matrix, **R**, in the 1D-Var calculation process. Fig.2-3 shows the observation errors calculated from the difference between corrected $T_{b[obs]}$ and $T_{b[sonde]}$ of each channel, and indicated that there is, however, a correlation between some channels. For the improvement of the 1D-Var calculation process, not only diagonal components but also off-diagonal components of the observation error covariance matrix, **R**, should be calculated from the errors of 138 cases (Fig.2-4a). According to the normalized correlation matrix (Fig.2-4b), there is high correlation among the oxygen band channels, and also among the water vapor band channels. There is little correlation between oxygen band channels and water vapor band channels.

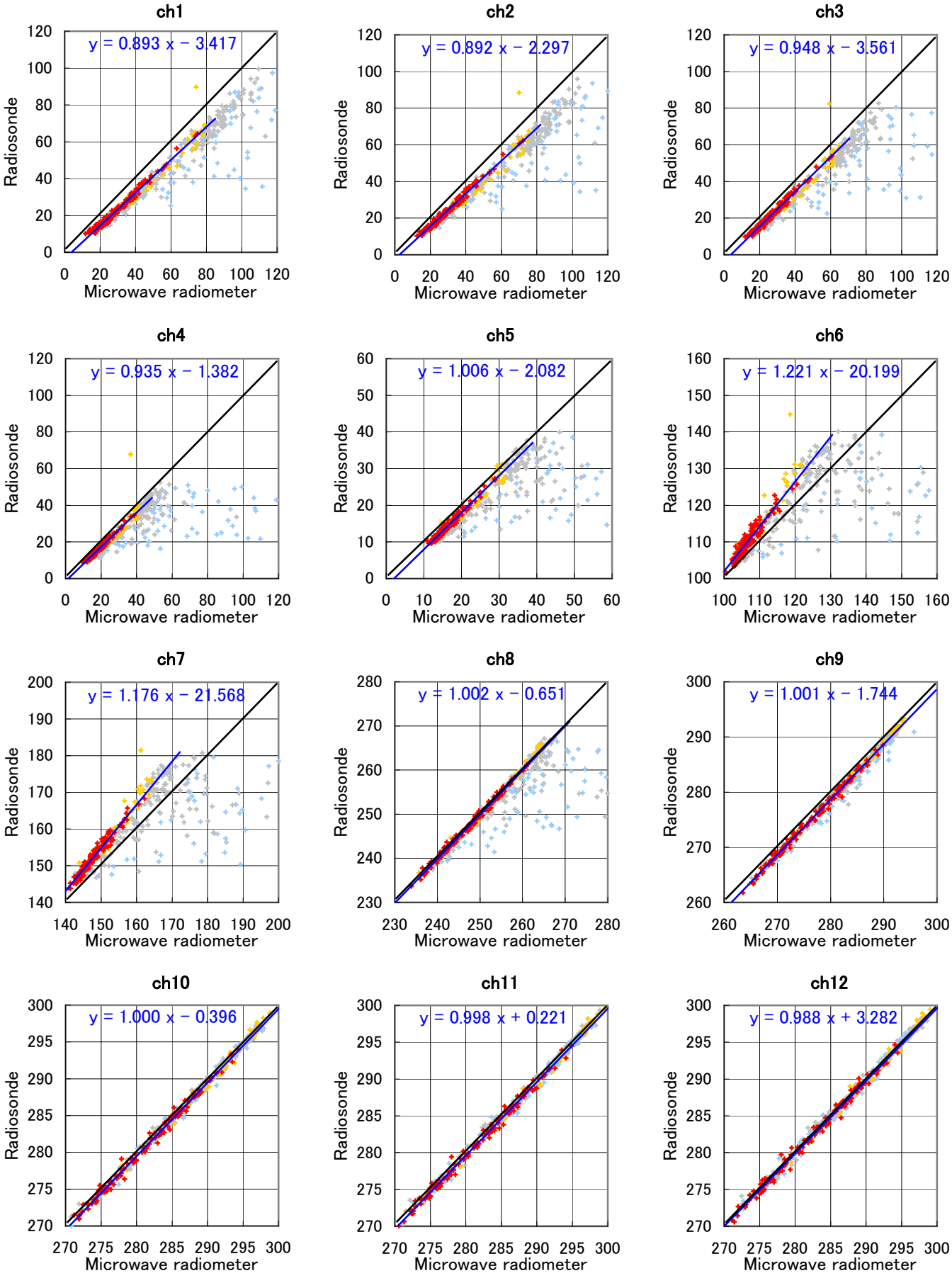

Fig.2-2. Scatter diagrams and regression lines of each channel.

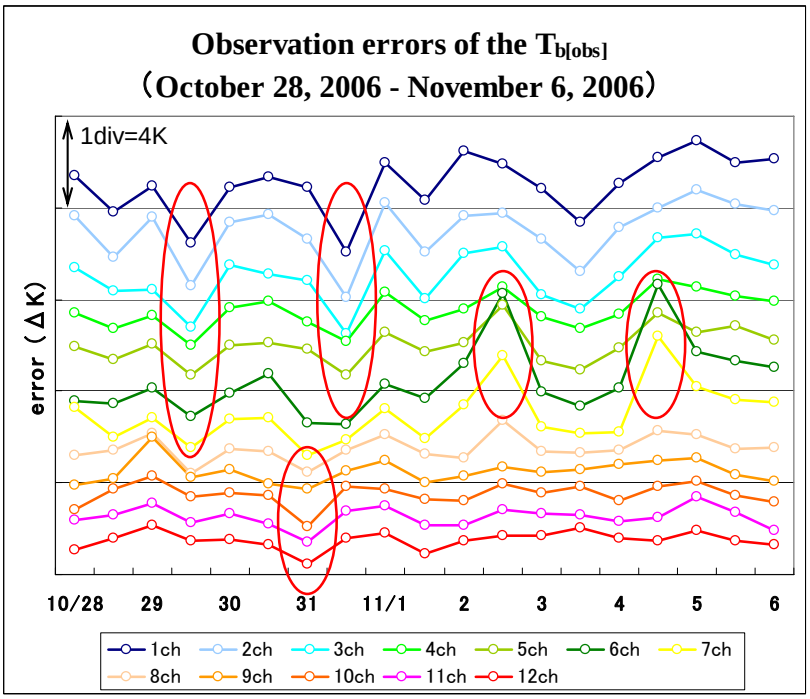

Fig.2-3. Observation errors calculated from the differences between corrected $T_{b[obs]}$ and $T_{b[sonde]}$ of each channel. There seem to be a correlation among the channels of close frequency.

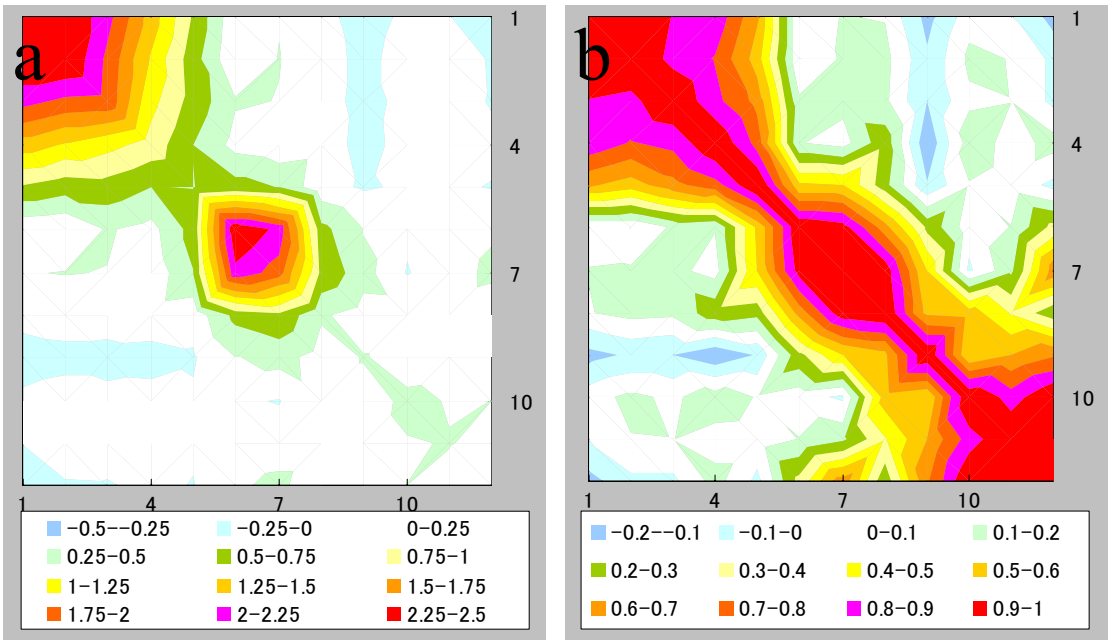

Fig.2-4. Observation error covariance matrix (a) and normalized correlation matrix (b).

High correlation is expected among all K and some V-band channels.

2-3. Background error covariance matrix

Same as the observation error covariance matrix, **R**, Yoshimoto (2007) also defined only diagonal components of the background error covariance matrix, **B**, in the 1D-Var calculation process. Off-diagonal components of the background error covariance matrix, **B**, as well as diagonal components, were calculated by using the difference between the forecast initiated six hours before the observation and that initiated three hours before the observation for all region of MSM from May 20, 2007 to November 30, 2007 (Fig.2-5, 2-6). Because these matrices have seasonal variations, they are calculated monthly.

2-4. Temperature and specific humidity on the surface

The radiometer measures pressure, temperature, relative humidity on the surface as well as $T_{b[obs]}$. To improve the accuracy of retrieved profiles, these observation data were included in the 1D-Var calculation process, and the cost function was redefined such as Eq.(2,2). T and w are the surface values of temperature and specific humidity. σ_t and σ_w are the standard deviation of the error of temperature and specific humidity respectively. x_{t1} and x_{w1} are the values of the lowest layer of the atmospheric state vector, **x**.

$$J'(\mathbf{x}) = J(\mathbf{x}) + \frac{(x_{t1} - T)^2}{2\sigma_t^2} + \frac{(x_{w1} - w)^2}{2\sigma_w^2} \quad (2,2)$$

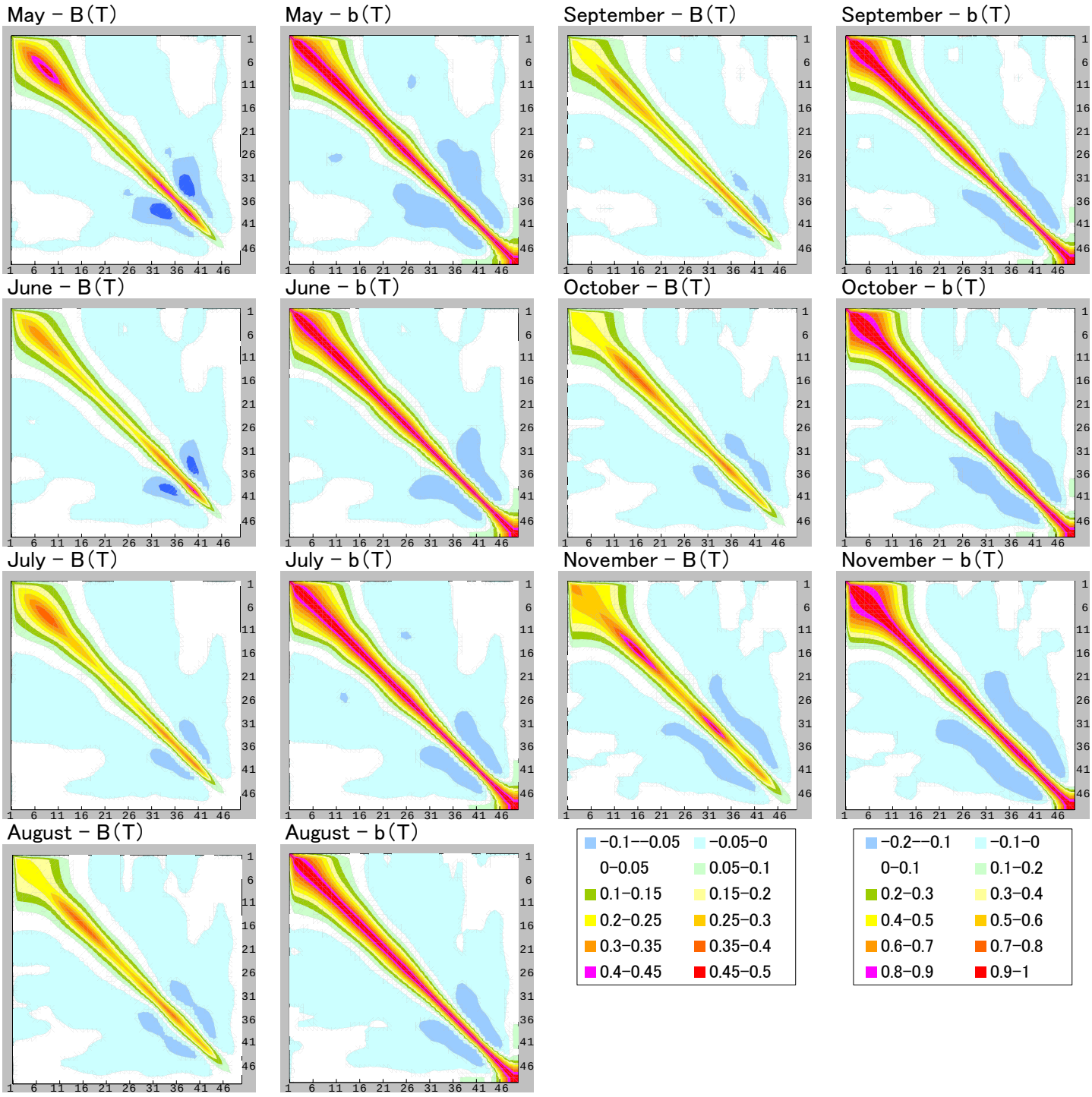

Fig.2-5. Background error covariance matrix, **B**, (temperature).

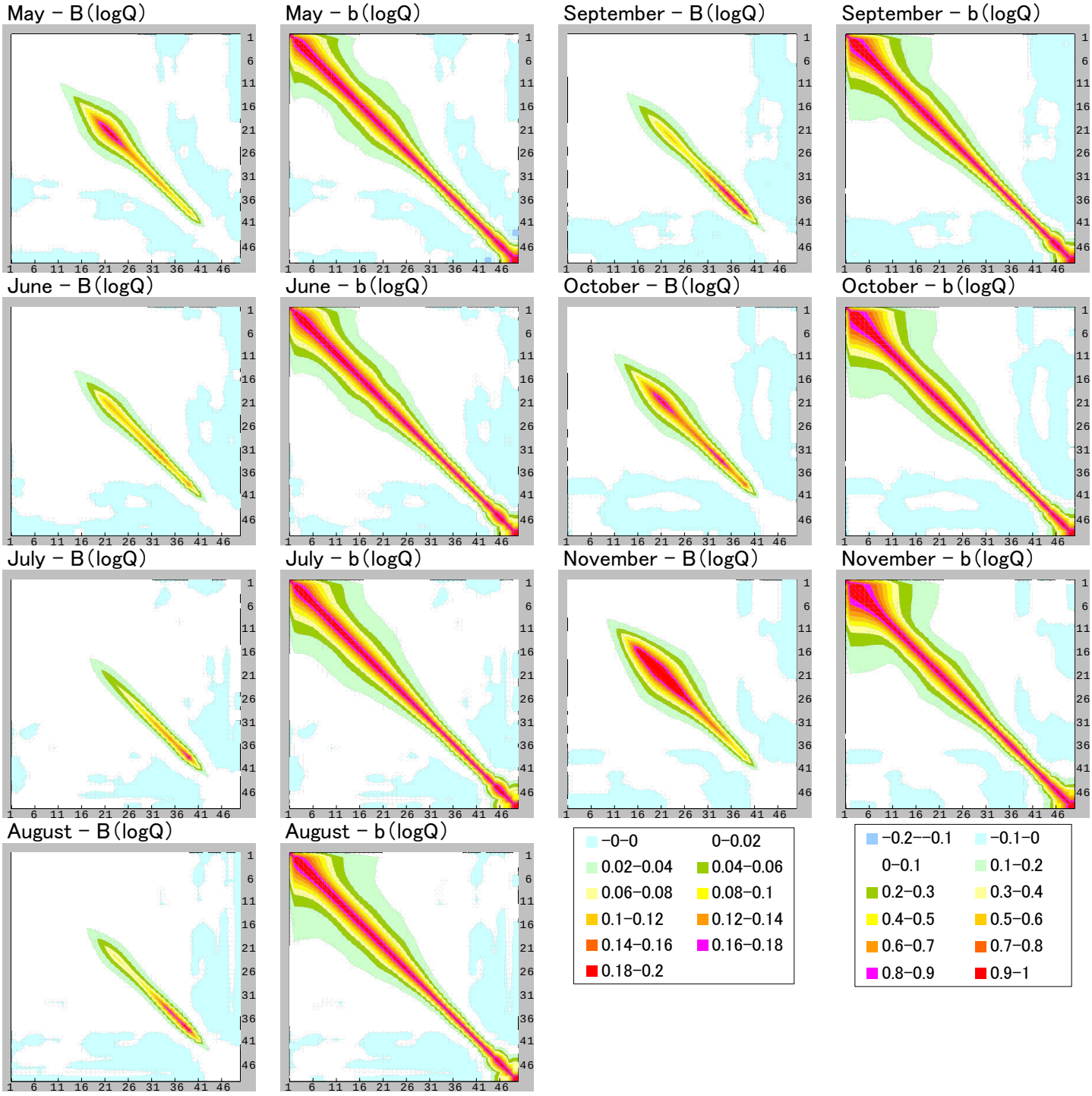

Fig.2-6. Background error covariance matrix, **B**, (natural log of the specific humidity).

3. Accuracy of the retrieved profiles by improved 1D-Var method

The 125 cases of vertical profiles under clear sky condition were retrieved by using the improved 1D-Var method described in section 2. The other 13 cases were not retrieved because the $T_{b[back]}$ which were calculated from background profiles were greatly different from the $T_{b[obs]}$ and the value of cost function was over a criteria.

The Mean Error (ME) of the retrieved temperature profiles from radiosonde is statistically better than that of backgrounds at altitudes of about 0-2 km, and the Root Mean Square Error (RMSE) of the retrieved profiles is also better than that of backgrounds at about 0-3 km (Fig.3-1). RMSE of the retrieved profiles is in particular better than that of analyzed profiles at 0-0.7 km.

The ME of the retrieved humidity profiles from radiosonde is better than that of backgrounds at about 0-6 km, and the RMSE of the retrieved profiles is better than that of backgrounds at about 0-4 km (Fig.3-2, Fig.3-3). However, RMSE of the retrieved profiles is not better than that of analyzed profiles.

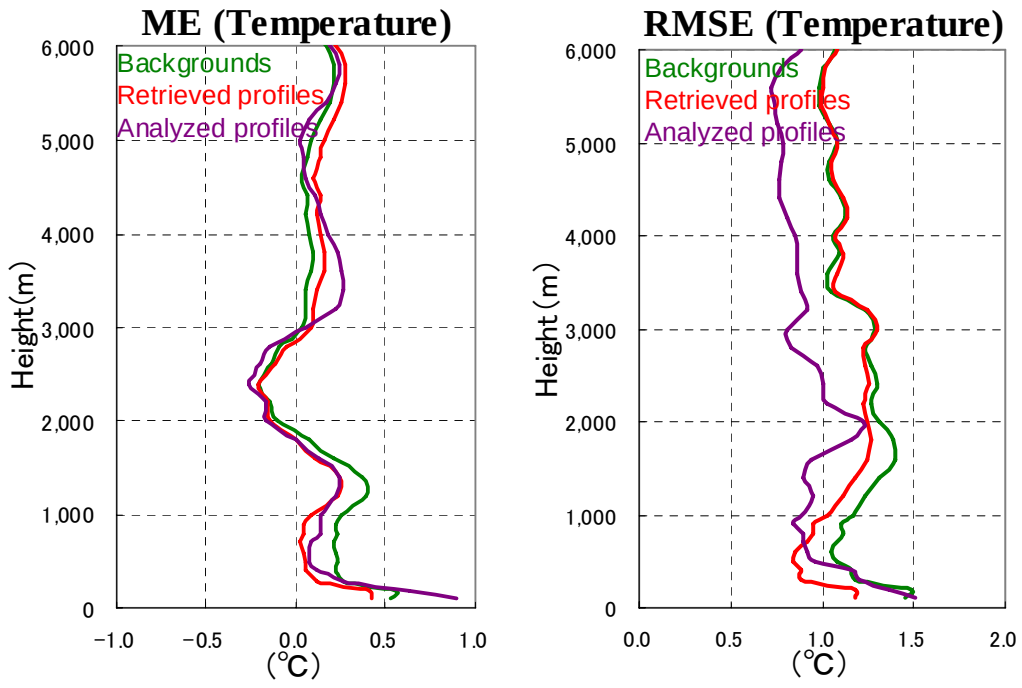

Fig.3-1. ME and RMSE of temperature profiles of 125 clear sky cases from April 19, 2006 to January 30, 2007. Green lines show the statistics of difference between backgrounds and radiosonde profiles, red lines show the difference between retrieved profiles and radiosonde profiles, and violet lines show the difference between analyzed profiles and radiosonde profiles.

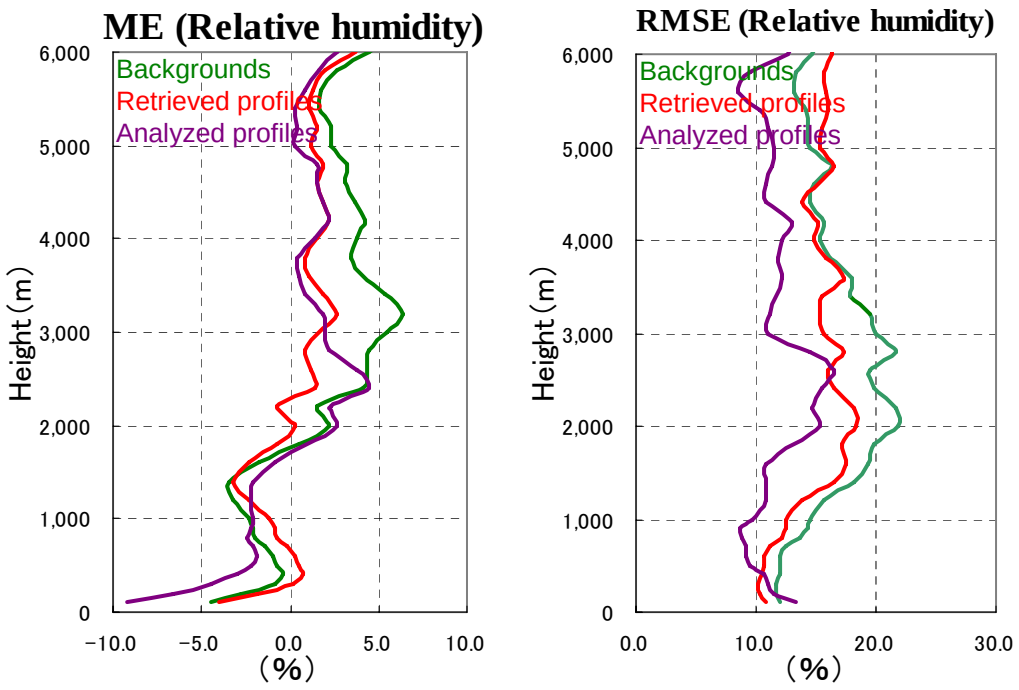

Fig.3-2. ME and RMSE of relative humidity profiles of 125 clear sky cases from April 19, 2006 to January 30, 2007.

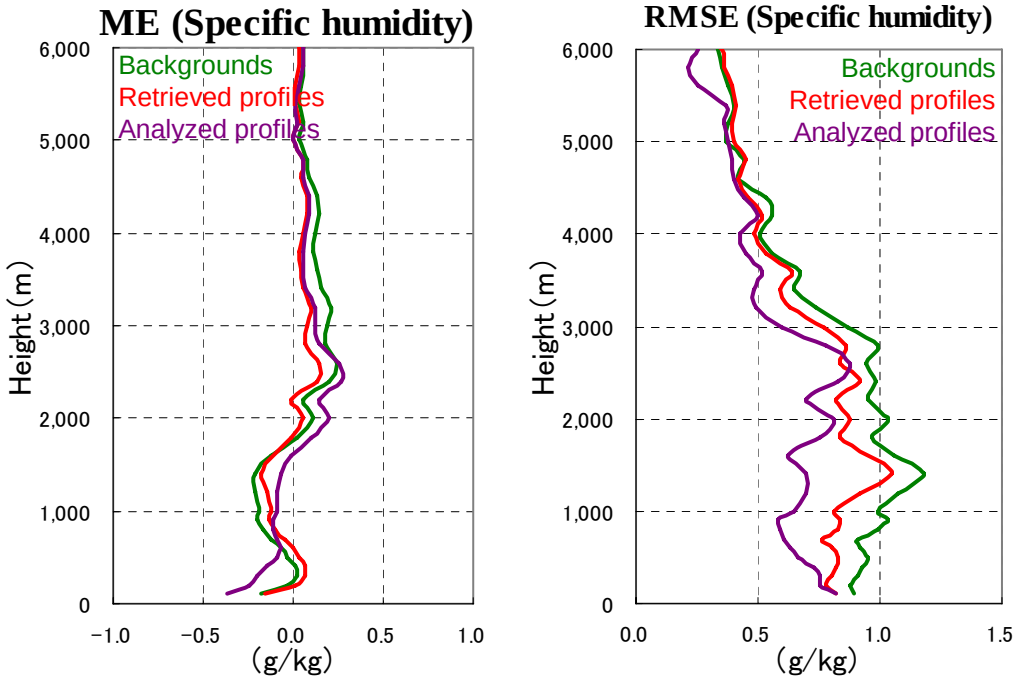

Fig.3-3. ME and RMSE of specific humidity profiles of 125 clear sky cases from April 19, 2006 to January 30, 2007.

Following these comparisons, the accuracy of the retrieved profiles was discussed from the viewpoint of brightness temperatures (Fig.3-4). In Fig.3-4, ME of $T_{b[1D\text{-}Var]}$ from $T_{b[sonde]}$ was better than that of $T_{b[back]}$ in water vapor band 1-5 channels. RMSE of $T_{b[1D\text{-}Var]}$ from $T_{b[sonde]}$ was also better than that of $T_{b[back]}$ and as good as that of $T_{b[anal]}$ in water vapor band channels. Here, $T_{b[1D\text{-}Var]}$ were calculated from retrieved profiles.

Figure.3-4 shows that the accuracy of $T_{b[1D\text{-}Var]}$ in water vapor band 1-5 channels are as good as that of $T_{b[anal]}$. However, the accuracy of the retrieved profiles is less than that of analyzed profiles. To discuss these results, it is helpful to consider "contribution profiles" shown in Fig.3-5. Fig.3-5 indicates that how much quantities does each altitude of atmosphere contribute to the total amount of downward radiation at ground level. Each line in Fig.3-5 is plotted by calculating the Radiative Transfer Equation on one certain actual observation. So these lines are variable under each atmospheric condition. But this figure is plotted under ordinary summer weather condition without raining. So we can discuss the general feature of atmospheric contribution to ground level radiation with this figure. In Fig.3-5, oxygen band 6-9 and 10-12 channels are sensitive to temperature at altitudes of about 0-4 km and 0-2 km respectively. Therefore, the information of 6-9 channels and that of 10-12 channels are used to retrieve the profiles of temperature at altitudes of about 0-4 km and 0-2 km.

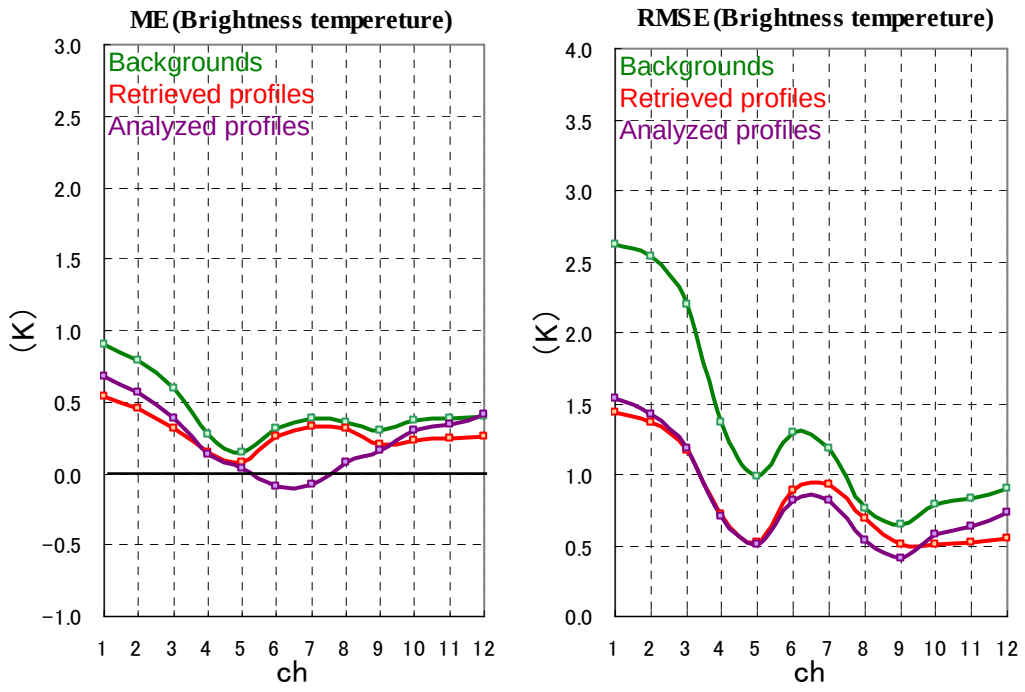

Fig.3-4. ME and RMSE of brightness temperatures of 125 clear sky cases from April 19, 2006 to January 30, 2007.

On the other hand, water vapor band 1-5 channels are sensitive to humidity at altitudes of about 0-6 km, and the characteristics of these sensitivities resemble each other in appearance. Then, the information of 1-5 channels are used to retrieve the profiles of humidity at altitudes of about 0-6 km. However, the information of $T_{b[obs]}$ doesn't work well to adjust the profiles of each altitude in the 1D-Var calculation process because of the similarity of the sensitivity characteristics. For the improvement of the specific humidity profiling, it is necessary to have water vapor channels which have various characteristics of the sensitivities in appearances.

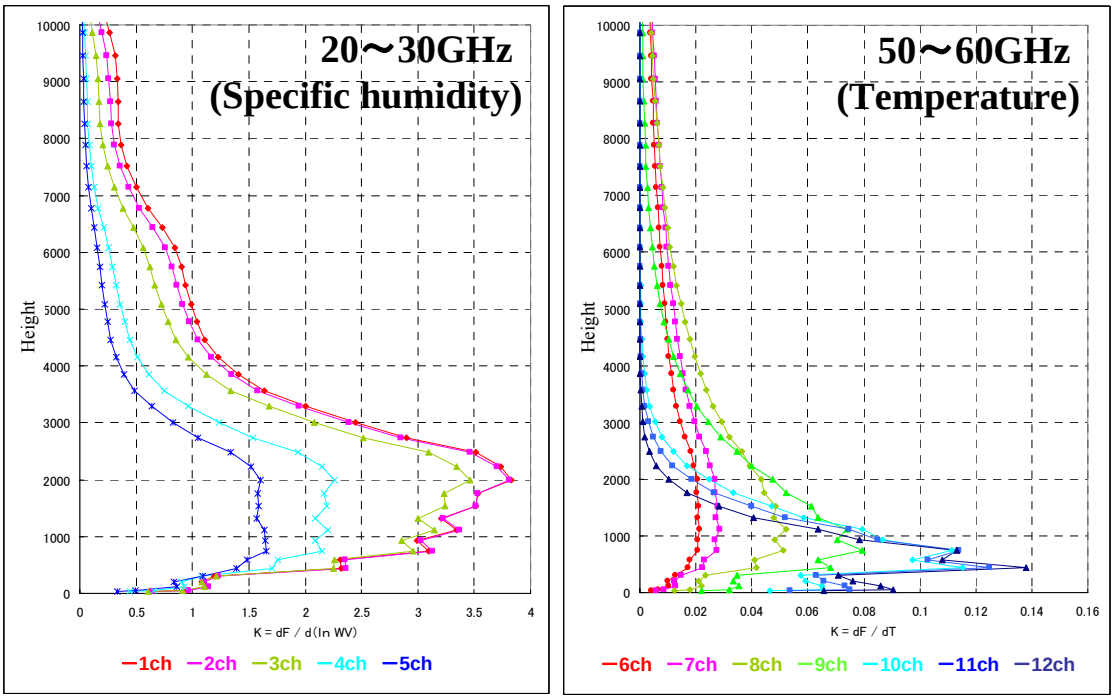

Fig.3-5. "Contribution profiles" of specific humidity and temperature.

4. Conclusions

In this study, some adjustments are made in the 1D-Var calculation process as follows.

1. Bias correcting for the $T_{b[obs]}$.
2. Calculating the error covariance matrices of the radiometer observation data and backgrounds in detail.
3. Including the surface observation data into the 1D-Var calculation process.

Then, the temperature profiles and the humidity profiles under clear sky condition were retrieved by improved 1D-Var method from April 19, 2006 to January 30, 2007. The results show that the accuracy of the retrieved temperature profiles and humidity profiles are statistically better than those of backgrounds at altitudes of about 0-3 km and 0-4 km respectively. Since these altitudes were consistent with the sensitivity characteristics of the

radiometer, it was found that the accuracy of the retrieved profiles was improved by the measured $T_{b[obs]}$.

On the other hand, because of the similarity of these sensitivity characteristics in water vapor channels, the information of $T_{b[obs]}$ is not adjusted well in the 1D-Var calculation process. For the improvement of the specific humidity profiling, it is necessary to have water vapor channels which have different profiles of the sensitivities in relation to altitudes.